New Short-Lived Isotope ^{221}U and the Mass Surface Near $N = 126$

J. Khuyagbaatar,[1,2,*] A. Yakushev,[1,2] Ch. E. Düllmann,[1,2,3] D. Ackermann,[2,†] L.-L. Andersson,[1] M. Block,[1,2,3] H. Brand,[2]
D. M. Cox,[4] J. Even,[1,‡] U. Forsberg,[5] P. Golubev,[5] W. Hartmann,[2] R.-D. Herzberg,[4] F. P. Heßberger,[1,2] J. Hoffmann,[2]
A. Hübner,[2] E. Jäger,[2] J. Jeppsson,[5] B. Kindler,[2] J. V. Kratz,[3] J. Krier,[2] N. Kurz,[2] B. Lommel,[2] M. Maiti,[6,§] S. Minami,[2]
A. K. Mistry,[4] Ch. M. Mrosek,[3] I. Pysmenetska,[2] D. Rudolph,[5] L. G. Sarmiento,[5] H. Schaffner,[2] M. Schädel,[2]
B. Schausten,[2] J. Steiner,[2] T. Torres De Heidenreich,[2] J. Uusitalo,[7] M. Wegrzecki,[8] N. Wiehl,[1,3] and V. Yakusheva[1]

[1]*Helmholtz Institute Mainz, 55099 Mainz, Germany*
[2]*GSI Helmholtzzentrum für Schwerionenforschung, 64291 Darmstadt, Germany*
[3]*Johannes Gutenberg-Universität Mainz, 55099 Mainz, Germany*
[4]*University of Liverpool, Liverpool L69 7ZE, United Kingdom*
[5]*Lund University, 22100 Lund, Sweden*
[6]*Saha Institute of Nuclear Physics, Kolkata 700064, India*
[7]*University of Jyväskylä, 40351 Jyväskylä, Finland*
[8]*The Institute of Electron Technology, 02-668 Warsaw, Poland*
(Received 14 July 2015; published 10 December 2015)

Two short-lived isotopes ^{221}U and ^{222}U were produced as evaporation residues in the fusion reaction ^{50}Ti + ^{176}Yb at the gas-filled recoil separator TASCA. An α decay with an energy of $E_\alpha = 9.31(5)$ MeV and half-life $T_{1/2} = 4.7(7)$ μs was attributed to ^{222}U. The new isotope ^{221}U was identified in α-decay chains starting with $E_\alpha = 9.71(5)$ MeV and $T_{1/2} = 0.66(14)$ μs leading to known daughters. Synthesis and detection of these unstable heavy nuclei and their descendants were achieved thanks to a fast data readout system. The evolution of the $N = 126$ shell closure and its influence on the stability of uranium isotopes are discussed within the framework of α-decay reduced width.

The shell structure of the atomic nucleus is one of the fundamental pillars of nature. As one consequence, spherically shaped nuclei with fully-filled proton and neutron shells at $Z, N = 2$, 8, 20, 28, 50, 82, and $N = 126$ have enhanced stability against any type of ground-state radioactive decay (alpha, beta, fission etc.) [1,2]. Many theoretical models are able to successfully describe the properties of these shell closures, and have thus attempted to predict the next heaviest magic numbers [3–7]. However, in contrast to the lighter magic numbers their results do not agree on the location of the next spherical doubly magic nucleus. Models within the macroscopic-microscopic approach often refer to $Z = 114$ and $N = 184$ [3–5], while microscopic ones predict various combinations (e.g., $Z = 120$, $N = 172$ [7] or $Z = 126$, $N = 184$ [6]). Direct tracing of these potential nuclear shell closures is limited by minute production rates, approaching the atom-per-month level for heaviest known elements up to $Z = 118$ [8]. Moreover neutron number $N = 184$ is presently not accessible experientially. Obtaining information about the evolution of nuclear shell closures in the heavy-element region is thus a prerequisite for gaining an improved understanding of superheavy nuclei.

Our current understanding of shell structure is well established, particularly in the case of nuclei along the valley of stability, where the magicity of shell closures is found. The robustness of these shell closures when going to

extremes in the proton-to-neutron ratio is less well studied, but the fading of classical shell closures has been observed in lighter regions of the chart of nuclei [2]. The $N = 126$ shell closure hosts the heaviest known stable doubly magic spherical nucleus, $^{208}_{82}$Pb$_{126}$, and is experimentally established up to protactinium ($Z = 91$), above which its evolution is yet poorly examined.

The evidence for the presence of the $N = 126$ shell closure above ^{208}Pb is based on systematic analyses of a limited amount of experimental data available to date like E_α and thus the deduced Q_α values, and half-life, $T_{1/2}$. More detailed information on nuclear structure can be obtained from the α-particle preformation probability inside the nucleus [9], which microscopically quantifies the stability against α decay. Different variables that are equivalent to the α-particle preformation probability in which both macroscopic observables Q_α and $T_{1/2}$ are simultaneously involved, can be deduced within different quantum-mechanical approaches [10,11]. Commonly, a reduced width for α decay, δ^2 [10], which takes into account the angular momentum of the emitted α particle, is used.

At and below $N = 126$, reduced widths of isotones of Po ($Z = 84$) to Pa are significantly lower than those of the $N = 128$–130 isotones located beyond the closed $N = 126$ shell [10–12]. This reflects the robustness of the $N = 126$ shell closure up to Pa and the effect of the semi-magic core with $N = 126$. The evolution of this closure towards higher

Z is yet unknown due to the absence of data on U isotopes with $N = 128$–130. U isotopes with $N = 124$–127 and $N \geq 131$ are known by their α decay [13–15]. For ^{222}U ($N = 130$), only a half-life is known, $T_{1/2} = 1.0^{+1.2}_{-0.4}$ μs, deduced from the observation of just three events [16]. The α-decay energies could not be measured as a result of the signals being summed (pileup) with those of the rapidly following α decays of the ^{218}Th daughter ($T_{1/2} = 0.117(9)$ μs [13]). Fast electronics have been successfully applied in recent decades to resolve similar pileup events in the charged particle spectroscopy of short-lived nuclei in regions of lighter elements (Refs. [17,18] and references therein).

Generally, the synthesis and detection of neutron-deficient isotopes of U (as well as heavier elements) in this region are challenging due to their low production rates and short half-lives [16,19]. An additional difficulty arises from the fusion reaction itself, as the compound nucleus fission and the evaporation of protons and/or α particles is by far dominant over neutron evaporation [19]. Thus, no new or improved data in this region of sub-μs isotopes carrying information on the $N = 126$ shell closure of elements above Pa have been measured in the last thirty years.

In this Letter, we report the first identification of the isotope ^{221}U and new data for ^{222}U. The known data on Po-U are discussed by means of α-decay systematics and thus help to shed light on the evolution of the $N = 126$ shell closure in U.

The experiment was carried out at the GSI Helmholtzzentrum für Schwerionenforschung, Darmstadt, Germany. The isotopes ^{221}U and ^{222}U were produced in the ^{50}Ti + ^{176}Yb reaction at the gas-filled TransActinide Separator and Chemistry Apparatus (TASCA) [20,21]. A pulsed (5 ms beam on and 15 ms beam off) ^{50}Ti^{12+} beam was accelerated by the UNIversal Linear ACcelerator (UNILAC) to energies in the range of 231–255 MeV in the center of the ^{176}YbF$_3$ targets. These correspond to excitation energies of 40–60 MeV in ^{226}U* where the maxima of $4n$ (^{222}U) and $5n$ (^{221}U) evaporation channels are predicted to occur according to the statistical fusion-evaporation code HIVAP [22]. Four target segments with average thicknesses of 0.45(5) mg/cm^2 (^{176}Yb) were mounted on a wheel which rotates synchronously to the beam pulses [23]. The magnets of TASCA were set to guide the evaporation residues (ERs) ^{221}U and ^{222}U with a magnetic rigidity of 1.66 Tm [24–26] to the center of the focal plane with an estimated efficiency of 50(5)%. The time of flight of the ^{221,222}U ERs through TASCA was estimated to be 0.53(6) μs.

ERs that do not decay in flight (through TASCA) were implanted into a double-sided silicon strip "stop detector" with 144 vertical and 48 horizontal 1-mm wide strips. A multiwire proportional counter (MWPC) was mounted in front of the stop detector to distinguish the genuine radioactive decay of implanted ERs from beam-related events. A detailed description of the TASCA focal plane detector is given in Ref. [21].

Signals from all the detectors were processed in a combined analog and digital (CANDI) data acquisition system comprising analog and digital branches. The shapes of the preamplified signals from the 48 horizontal strips (n^+ side) were recorded in 50 μs-long traces by analog-to-digital converters with 60 MHz sampling [27]. The trace length was selected to be longer than the dead time of the analog branch of $\approx$35 μs. Energy resolutions (FWHM) of individual vertical strips of the stop detector coupled to the analog branch were about 30 keV for 8.7-MeV α particles. The amplitudes, i.e., energies of signals stored in traces were extracted by using different types of software algorithms depending on the multiplicity of the recorded signals [28]. The best resolutions, about 40 keV, were achieved for 8.7-MeV α particles that were registered as single events in the traces. The best energy resolutions of multiple α events stored in a single trace with time differences down to 1 μs and 0.17 μs were $\approx$110 keV and $\approx$180 keV, respectively.

Half-lives known for ^{222}U and its daughter ^{218}Th and predicted for ^{221}U are much shorter [13] than the 50 μs trace-length of CANDI. Thus, their radioactive decay signature is registered in digital traces of implantation signals (ER-like). The analysis procedure thus consists of two main steps.

(i) A correlation analysis of the analog data, searching for ER-α chains requiring that both the ER-like and the α-like events (7–18 MeV) occurred in the same pixel of the stop detector within 20 s. The results of the correlation analysis are shown in Fig. 1. The implantation of ^{214}Ra, ^{215}Ra, ^{217}Th, and ^{214}Fr was identified by their known
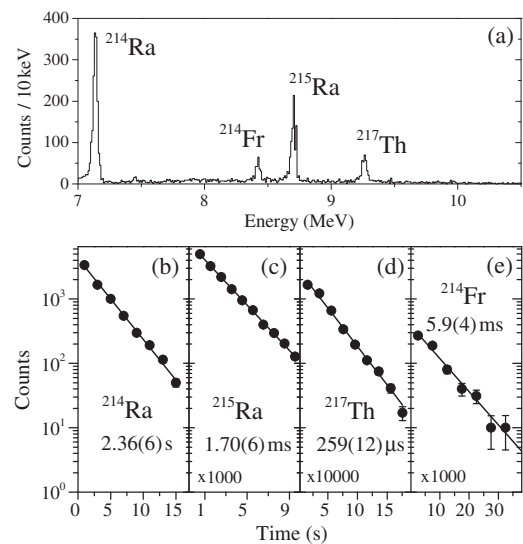

FIG. 1. Results from a correlation analysis of the type ER-α within 20 s: (a) Spectrum of correlated α particles registered at a bombarding energy of 239 MeV and (b)–(d) total decay curves of the implanted nuclei. (e) Decay curve of ^{214}Fr identified in the correlation analysis of type ER-α(7–18 MeV)-α(^{214}Fr).
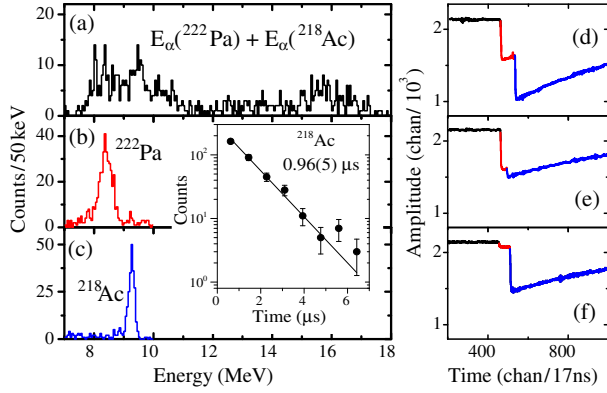
FIG. 2 (color online). Identification spectra for the separation of pileup events originating from the decay chains ER-$\alpha(7-18$ MeV)-$\alpha(^{214}$Fr). (a) Energy spectrum from the analog part of the data. (b),(c) Energy spectra of events deduced from the digital traces. Examples of some pileup traces: (d) two α particles with full energies, (e) and (f) for traces where the second and first α particle, respectively, escaped in the backward direction and deposited only partial energy in the stop detector.

FIG. 3. Energy spectra and decay curves of α particles emitted from ^{219}Th, ^{218}Th, ^{222}U, and ^{221}U. The data were extracted from the digital data branch. In the case of ^{218}Th both double and triple-signaled traces from ER-$\alpha(^{214}$Ra) were used. All traces with time differences down to 100 ns between the preceding signal and α decay were used.

α-decay properties [13], and the corresponding ERs were assigned for each event.

(ii) Traces of all ERs correlated to a subsequent α decay of ^{214}Ra and ^{217}Th, which are members of the α-decay chains originating from ^{222}U and ^{221}U, respectively, were checked event by event for the presence of multiple signals.

In the cases of ^{217}Th and ^{214}Fr, an additional ER-α-α correlation analysis was performed to reconstruct the full pattern of the α-decay chain. As an example, ^{214}Fr was found to be the last member of the ER-$\alpha(7$-18 MeV)-$\alpha(^{214}$Fr) chain with $T_{1/2} = 5.9(4)$ ms (see Fig. 1). An energy spectrum (analog branch) of the second member with $T_{1/2} = 3.5(1)$ ms is shown in Fig. 2(a). To resolve apparent pileup events, the digital traces were analyzed in the second step. Different examples of such events are presented in Figs. 2(d)–2(f). The energy spectra of the two signals allowed the separate peaks to be clearly resolved, which correspond to known α-decay energies of ^{222}Pa and ^{218}Ac [13]. Time differences between those signals yield $T_{1/2} = 0.96(5)$ μs, which agrees well with the literature data of ^{218}Ac [13]. Thus, the origin of the α decay of ^{214}Fr was attributed to the implantation of ^{222}Pa produced as an ER via the $p3n$ deexcitation channel from the compound nucleus ^{226}U*. The same digital-trace analysis was used for the extraction of α-decay properties of all other short-lived nuclei.

Significant amounts of ER traces correlated to $\alpha(^{215}$Ra) were stored with double signals. A resolved energy spectrum of the second signal and the decay curve extracted from the time difference of these signals (shown in Fig. 3) is in good agreement with the literature data for ^{219}Th [13]. No triple signals, which would correspond to the implantation of ^{223}U ($T_{1/2} = 55(10)$ μs [13]) from the $3n$ channel, were detected.
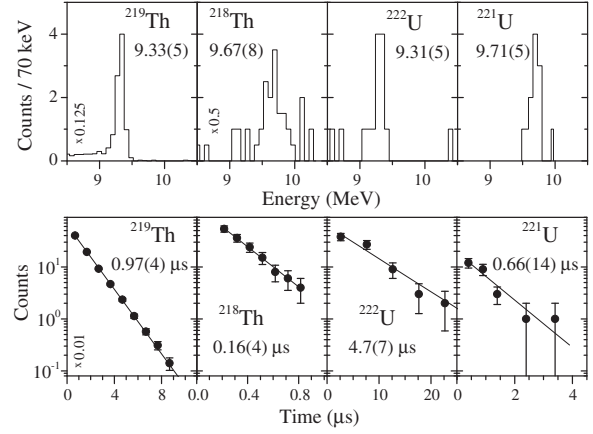
Traces with two and three signals were detected for ERs followed by $\alpha(^{214}$Ra). Traces with two signals and with very short time differences leading to $T_{1/2} = 0.16(4)$ μs (see Fig. 3) between the signals were assigned to the implantation and α decay of ^{218}Th ($T_{1/2} = 0.117(9)$ μs [13]) produced in the $\alpha 4n$ channel.

Eighty-one ER traces containing three signals were unambiguously attributed to the implantation of ^{222}U followed by α decays of ^{222}U and ^{218}Th. One such trace is shown in Fig. 4. A half-life of 4.7(7) μs and an energy of 9.31(5) MeV were deduced for the α decay of ^{222}U (see Fig. 3).

Twenty-six ER traces followed by subsequent α decays of ^{217}Th and ^{213}Ra were stored with double signals and are attributed to the implantation and α decay of the hitherto unknown ^{221}U (see Fig. 4). A half-life of 0.66(14) μs and an α-particle energy of 9.71(5) MeV were deduced (see Fig. 3) for this isotope.

The most favored α transitions in nuclei with $N = 129$ proceed through the same $\nu 2g_{9/2}$ orbital in the mother and
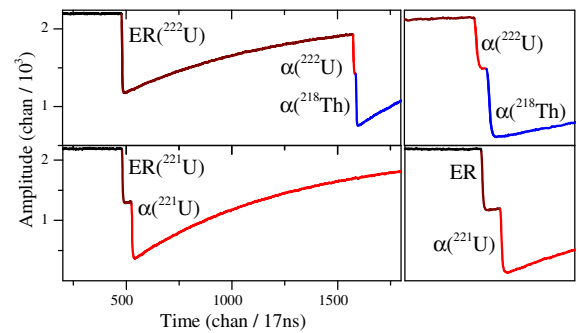

FIG. 4 (color online). Examples of traces where ^{222}U and ^{221}U were registered. Right panel: Enlarged figures of rapidly correlated signals.

daughter nuclei. Thus, the observed α decay in ^{221}U is attributed to such a transition. The $(9/2^+)$ state is tentatively assigned to the ground state of ^{221}U based on systematics [13,14]. Alpha decays of both ^{221}U and ^{222}U are in good agreement with Q_α [29] and $T_{1/2}$ systematics [14].

The new α-decay data on ^{221}U and ^{222}U together with literature values for Po-Th ([13,15]) allow us to construct the tendencies of δ^2 in the $N = 129, 130$ isotones up to U, where the $\pi(1h_{9/2})$ orbital is fully filled. The deduced δ^2 values for the $N = 124, 126–130$ isotones are shown in Fig. 5. In the case of the $N = 129$ isotones, only α transitions populating the same single-neutron states in the daughter nuclei were taken. For the cases at $N = 127$, the α transition proceeds between different initial $\nu(2g_{9/2})^1$ and final $\nu(3p_{1/2})^{-1}$ configurations. Thus we use $\Delta\ell = 0$ for $N = 129$ and $\Delta\ell = 5$ for $N = 127$. Up to Th ($Z = 90$), the δ^2 values for the $N = 124, 128–130$ isotones are larger than the $N = 126, 127$ ones, which clearly shows a strong effect of the $N = 126$ shell closure. At the same time, the δ^2 values for the $N = 126, 127$ isotones, which are known up to U, smoothly rise with increasing Z, indicating a weakening of the semi-magic core with $N = 126$. For the $N = 129, 130$ isotones, where our new data allow extending the systematics up to U, the δ^2 values decrease in contrast to the trend seen in the $N = 126, 127$ isotones. The sudden increase of δ^2 values when crossing the $N = 126$ shell closure seen in lighter elements with even A is no longer present at $Z = 92$. In odd-A nuclei, the gap is still

persisting at $Z = 92$, in contrast to the even-A case. Essentially, α decay of the even-even nuclei, where all nucleons are paired, provides better information on their structure compared to odd-A ones, where α decay is strongly influenced by their unpaired nucleon.

The above observed feature for even-A nuclei indicates a weakening of the $N = 126$ shell stabilization effect for U, which can be inferred even in the absence of data on ^{220}U ($N = 128$). In addition, δ^2 values for the $N = 124$ isotones show again a notable discrepancy in U. The smallest δ^2 value is found in ^{216}U ($N = 124$), which can be argued as having a more stabilized core than the semi-magic ^{218}U ($N = 126$).

A weakening of the $N = 126$ shell closure can also be seen in the reduction of the neutron-shell gap in elements above Pb ($Z = 82$). The neutron-shell gap, G_n, between the last-occupied and first-valence orbitals around $N = 126$ can be calculated as

$$G_n(Z, 126) = 2B(Z, 126) - B(Z, 125) - B(Z, 127) \quad (1)$$

using the known (except ^{217}U) binding energies, B [2,29]. These gaps are shown in Fig. 5 (bottom panel) where we compare experimental data ([29]) with those obtained using two different theoretical models (FRDM95 [4], HFB26 [30]). A reduction of G_n as a function of Z for heavier elements is observed in the experimental data, supporting the above discussed weakening of the shell closure inferred on the basis of the trends of δ^2 values. G_n values are significantly reduced when crossing $Z = 82$, which can be attributed to the loss of the magic $Z = 82$ partner, which leads to less stable semi-magic nuclei with ^{218}U being the most unstable $N = 126$ isotone known to date.

Two theoretical models, FRDM95 and HFB26, were selected as representatives of the macroscopic-microscopic and microscopic approaches, respectively. The macroscopic-microscopic approach is based on corrections of calculated liquid-droplet masses to the shell structure, while the microscopic ones take into account the interactions between the nucleons with differently parametrized effective forces for the solution of the many-body quantum equations within particular approximations such as Hartree-Fock-Bogoliubov with Skyrme force (HFB26). The Finite-Range Droplet Model (FRDM95) predicts well the G_n values around the doubly magic ^{208}Pb, but fails to describe the decreasing trend for heavier elements. On the other hand, the HFB26 model does not perform as well around ^{208}Pb, but predicts the reduction of G_n towards heavier elements better. This shows the importance of interactions between the valence nucleons for the evolution of the shell closure.

The anomalous behavior observed in U thus may hint at significant changes in its structure due to nucleon-nucleon interactions, for instance the presence of non-negligible deformation as discussed theoretically in Ref. [31]. To date, no experimental data on deformations of
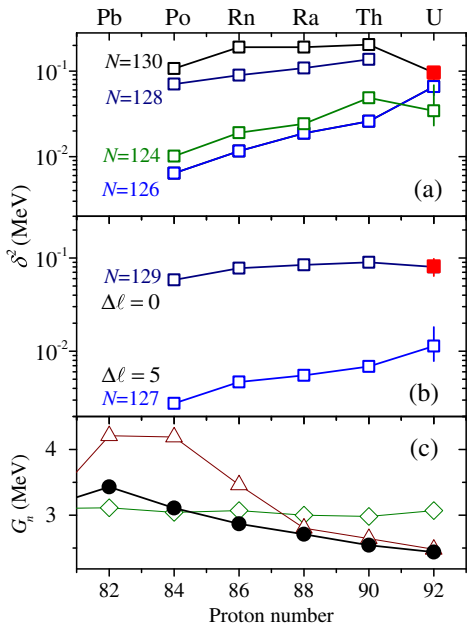

FIG. 5 (color online). Reduced α-decay widths (δ^2, [10]) of even-A (a) and odd-A (b) isotopes, and (c) neutron-shell gaps (G_n, [2]) of Po-U as a function of the Z. Errors originating solely from half-lives are given for U. (c) Experimental data (full dots) [29] are compared to FRDM95 (open diamonds) [4] and HFB26 (open triangles) [30] calculations. See text for details.

$N = 124$–130 isotones are available for Po-U, except for ^{218}Ra ($N = 130$), where the quadrupole deformation is 0.091(4) [13].

In conclusion, we report the discovery of the isotope ^{221}U as well as unambiguous identification of ^{222}U. Half-lives of 4.7(7) μs and 0.66(14) μs and α-particle energies of 9.31(5) MeV and 9.71(5) MeV were measured for ^{222}U and ^{221}U, respectively. These were produced in the fusion-evaporation reaction ^{50}Ti+^{176}Yb with maximum cross sections of a few nanobarns at 47 and 54 MeV excitation energies of ^{226}U* [28]. The comparative analysis of the reduced widths and neutron-shell gaps of the Po-U isotopes shows a significant weakening of the influence of the $N = 126$ shell closure in U. Our findings motivate further investigations of the $N = 126$ shell closure by synthesizing hitherto unknown nuclei, and by detailed studies of U. The experimental technique applied in the present work allows the identification of short-lived activities in a wide range of the nuclear chart and particularly for the still unobserved ^{220}U for which, though, the predicted half-life is only several tens of ns [14] and hence too short for surviving the flight time through TASCA. A preferable way to synthesize this isotope would be via its significantly longer lived [32] α-decay precursor ^{224}Pu.

---

*J.Khuyagbaatar@gsi.de

†Present address: GANIL, CEA/DSM-CNRS/IN2P3, Bd Henri Becquerel, BP 55027, F-14076 Caen Cedex 5, France.

‡Present address: TRIUMF, 4004 Wesbrook Mall Vancouver, BC, V6T 2A3, Canada.

§Present address: Indian Institute of Technology Roorkee, Roorkee 247667, India.

[1] M. Pfützner, M. Karny, L. V. Grigorenko, and K. Riisager, Rev. Mod. Phys. **84**, 567 (2012).

[2] O. Sorlin and M.-G. Porquet, Prog. Part. Nucl. Phys. **61**, 602 (2008).

[3] A. Sobiczewski, F. A. Gareev, and B. N. Kalinkin, Phys. Lett. **22**, 500 (1966).

[4] P. Moller, J. R. Nix, W. D. Myers, and W. J. Swiatecki, At. Data Nucl. Data Tables **59**, 185 (1995).

[5] I. Muntian, Z. Patyk, and A. Sobiczewski, Phys. At. Nucl. **66**, 1015 (2003).

[6] K. Rutz, M. Bender, T. Bürvenich, T. Schilling, P.-G. Reinhard, J. A. Maruhn, and W. Greiner et al., Phys. Rev. C **56**, 238 (1997).

[7] W. Zhang, J. Meng, S. Q. Zhang, L. S. Geng, and H. Toki, Nucl. Phys. A **753**, 106 (2005).

[8] J. H. Hamilton, S. Hofmann, and Y. T. Oganessian, Annu. Rev. Nucl. Part. Sci. **63**, 383 (2013).

[9] H. J. Mang, Annu. Rev. Nucl. Sci. **14**, 1 (1964).

[10] J. O. Rasmussen, Phys. Rev. **113**, 1593 (1959).

[11] A. N. Andreyev et al., Phys. Rev. Lett. **110**, 242502 (2013).

[12] K. S. Toth et al., Phys. Rev. C **60**, 011302 (1999).

[13] http://www.nndc.bnl.gov/ensdf/.

[14] G. Audi, F. G. Kondev, M. Wang, B. Pfeiffer, X. Sun, J. Blachot, M. MacCormick, Chin. Phys. C **36**, 1157 (2012).

[15] L. Ma et al., Phys. Rev. C **91**, 051302(R) (2015).

[16] R. Hingmann, H.-G. Clerc, C.-C. Sahm, D. Vermeulen, K.-H. Schmidt, and J. G. Keller, Z. Phys. A **313**, 141 (1983).

[17] J. Basilio Simões and C. M. B. A. Correia, Nucl. Instrum. Methods Phys. Res., Sect. A **422**, 405 (1999).

[18] S. N. Liddic et al., Phys. Rev. Lett. **97**, 082501 (2006).

[19] K. Nishio, H. Ikezoe, S. Mitsuoka, and J. Lu, Phys. Rev. C **62**, 014602 (2000).

[20] A. Semchenkov et al., Nucl. Instrum. Methods Phys. Res., Sect. B **266**, 4153 (2008).

[21] J. M. Gates et al., Phys. Rev. C **83**, 054618 (2011).

[22] W. Reisdorf, Z. Phys. A **300**, 227 (1981).

[23] E. Jäger, H. Brand, Ch. E. Düllmann, J. Khuyagbaatar, J. Krier, M. Schädel, T. Torres, and A. Yakushev, J. Radioanal. Nucl. Chem. **299**, 1073 (2014).

[24] K. E. Gregorich, Nucl. Instrum. Methods Phys. Res., Sect. A **711**, 47 (2013).

[25] J. Khuyagbaatar et al., Nucl. Instrum. Methods Phys. Res., Sect. A **689**, 40 (2012).

[26] J. Khuyagbaatar, V. P. Shevelko, A. Borschevsky, Ch. E. Düllmann, I. Yu. Tolstikhina, and A. Yakushev, Phys. Rev. A **88**, 042703 (2013).

[27] N. Kurz et al., GSI Scientific Report 252, 2012; J. Hoffmann et al., GSI Scientific Report 253, 2012.

[28] J. Khuyagbaatar et al. (to be published).

[29] M. Wang, G. Audi, A. H. Wapstra, F. G. Kondev, M. MacCormick, X. Xu, and B. Pfeiffer, Chin. Phys. C **36**, 1603 (2012).

[30] S. Goriely, N. Chamel, and J. M. Pearson, Phys. Rev. C **88**, 024308 (2013).

[31] S. V. Tolokonnikov, I. N. Borzov, M. Kortelainen, Yu. S. Lutostansky, and E. E. Sape, J. Phys. G **42**, 075102 (2015).

[32] P. Möller, J. R. Nix, and K.-L. Kratz, At. Data Nucl. Data Tables **66**, 131 (1997).